Molecular Biology of the Cell
Vol. 19, 5131–5142, December 2008

Voa1p Functions in V-ATPase Assembly in the Yeast Endoplasmic Reticulum

Margret Ryan,* Laurie A. Graham,* and Tom H. Stevens

Institute of Molecular Biology, University of Oregon, Eugene, OR 97403

Submitted June 20, 2008; Revised August 20, 2008; Accepted September 8, 2008
Monitoring Editor: Sandra Lemmon

The yeast *Saccharomyces cerevisiae* vacuolar ATPase (V-ATPase) is a multisubunit complex divided into two sectors: the V_1 sector catalyzes ATP hydrolysis and the V_0 sector translocates protons, resulting in acidification of its resident organelle. Four protein factors participate in V_0 assembly. We have discovered a fifth V_0 assembly factor, Voa1p (YGR106C); an endoplasmic reticulum (ER)-localized integral membrane glycoprotein. The role of Voa1p in V_0 assembly was revealed in cells expressing an ER retrieval-deficient form of the V-ATPase assembly factor Vma21p (Vma21pQQ). Loss of Voa1p in *vma21QQ* yeast cells resulted in loss of V-ATPase function; cells were unable to acidify their vacuoles and exhibited growth defects typical of cells lacking V-ATPase. V_0 assembly was severely compromised in *voa1 vma21QQ* double mutants. Isolation of V_0–Vma21p complexes indicated that Voa1p associates most strongly with Vma21p and the core proteolipid ring of V_0 subunits c, c′, and c″. On assembly of the remaining three V_0 subunits (a, d, and e) into the V_0 complex, Voa1p dissociates from the now fully assembled V_0–Vma21p complex. Our results suggest Voa1p functions with Vma21p early in V_0 assembly in the ER, but then it dissociates before exit of the V_0–Vma21p complex from the ER for transport to the Golgi compartment.

INTRODUCTION

The V-type proton-translocating ATPase (V-ATPase) is a ubiquitous multisubunit protein complex present in all eukaryotic cells from yeast to humans (Beyenbach and Wieczorek, 2006). In eukaryotes, the V-ATPase is localized to the membranes of intracellular organelles such as Golgi, endosomes, vesicles, and vacuole or lysosome (Forgac, 2007). The function of the V-ATPase complex is to translocate protons across a lipid bilayer by an ATP-driven rotary mechanism (Hirata *et al*., 2003; Imamura *et al*., 2003; Yokoyama *et al*., 2003). The ATP-driven acidification of the lumen of these organelles by the resident V-ATPase plays a role in regulating a diverse range of cellular processes such as receptor–ligand interactions, accumulation of neurotransmitter in synaptic vesicles, and intracellular trafficking (Forgac, 2007). In addition to the localization throughout the Golgi/endosome/lysosomal network, the V-ATPase also can be found on the plasma membrane in specialized cells such as osteoclasts, kidney cells, and neurons in which it functions in bone resorption, acid–base balance, and neurotransmitter accumulation (Forgac, 2007).

The best-characterized member of the V-ATPase family is present in the yeast *Saccharomyces cerevisiae* (Graham *et al*., 2003; Kane, 2006), because the V-ATPase is essential for cell viability in all eukaryotes except fungi. In yeast, the V-ATPase acidifies the lumen of the vacuole, Golgi, and endosomes by establishing an ATP-driven proton gradient across the membrane. In turn, various membrane-bound ion transporters/proton exchangers use this gradient to sequester metal ions to the vacuole and other cellular organelles. The combined action of the V-ATPase and membrane transporters plays a key role in maintaining cellular homoeostasis in yeast (Kane, 2006).

The V-ATPase complex can be functionally separated into two subcomplexes: the V_1 domain involved directly in ATP hydrolysis and the V_0 domain responsible for the translocation of protons across a membrane bilayer. The V-ATPase complex in yeast is composed of 14 integral and peripheral membrane subunits. The V_0 domain is assembled in the endoplasmic reticulum (ER) and is composed of subunits a, c, c′, c″, d, and e encoded by the yeast genes *VPH1* or *STV1*, *VMA3*, *VMA11*, *VMA16*, *VMA6* and *VMA9*, respectively. The V_1 domain contains subunits A, B, C, D, E, F, G, and H encoded by the yeast genes *VMA1*, *VMA2*, *VMA5*, *VMA8*, *VMA4*, *VMA7*, *VMA10*, and *VMA13*. Subunits A, B, E, G, and c are present in the V-ATPase at more than one copy per complex (Powell *et al*., 2000; Ohira *et al*., 2006; Kitagawa *et al*., 2008).

In yeast, there are two populations of V-ATPase complexes that are identical except for the subunit a isoform present in each complex (Manolson *et al*., 1992, 1994). The presence of the Vph1p subunit a isoform directs localization of the V-ATPase complex to the membrane of the vacuole, and inclusion of the Stv1p subunit a isoform results in the retention of the V-ATPase complex on Golgi and endosomal membranes (Manolson *et al*., 1994). The targeting information determining the cellular localization of the Vph1p and Stv1p containing V-ATPase complexes resides in the N-terminal half of each subunit a isoform (Kawasaki-Nishi *et al*., 2001).

This article was published online ahead of print in *MBC in Press* (http://www.molbiolcell.org/cgi/doi/10.1091/mbc.E08–06–0629) on September 17, 2008.

* These authors contributed equally to this work.

Address correspondence to: Tom H. Stevens (stevens@molbio.uoregon.edu).

Abbreviations used: DAPI, 4′,6-diamidino-2-phenylindole; GFP, green fluorescent protein; ER, endoplasmic reticulum; HA, hemagglutinin; V-ATPase, vacuolar-type proton-translocating ATPase; YEPD, yeast extract peptone dextrose.

Yeast cells lacking a functional V-ATPase display a characteristic set of growth phenotypes, collectively referred to as the Vma$^-$ phenotype; they are able to grow on rich medium buffered to pH 5.0 but are unable to grow on more alkaline media buffered to pH 7.5 or in the presence of elevated levels of calcium (Kane, 2006). V-ATPase–deficient cells are unable to acidify their vacuoles, a phenomenon that can be observed at the cellular level by failure to accumulate the fluorescent dye quinacrine in the lumen of the vacuoles (Weisman *et al.*, 1987). Failure to assemble the V_1 subcomplex due to loss of any one of the V_1 subunits does not affect the assembly and targeting of the V_0 subcomplex in yeast (Graham *et al.*, 2003). Cells lacking both Vph1p and Stv1p or any one of the other V_0 subunits, fail to assemble a complete V_0 subcomplex, and this partially assembled complex does not exit the ER. Yeast cells lacking any of the other V_0 subunits (except Stv1p) exhibit reduced cellular levels of Vph1p due to increased turnover of this subunit when it is unable to assemble properly into the V_0 subcomplex and exit the ER.

In addition to proteins that comprise the fully functional V-ATPase complex, proteins have been identified and characterized that play a role in the assembly of the V-ATPase. Although the V_1 and V_0 subcomplexes are capable of assembling independently in cells, there is evidence that V_1 subunits associate very early with V_0 subunits in the ER (Kane *et al.*, 1999; Kane, 2006). One interpretation of these data are that although V_1 subunit association is not required for V_0 assembly in the ER, the normal pathway for V-ATPase assembly could involve association of certain V_1 subunits with components of the V_0 subcomplex during its assembly in the ER. Intriguingly, the *r*egulator of the *A*TPase of *v*acuolar and *e*ndosomal membranes (RAVE) complex (Seol *et al.*, 2001) is required for the stable association of the V_1 domain with the V_0 domain during biosynthesis (Smardon *et al.*, 2002) and for the glucose-regulated reassembly of the V_1 and V_0 domains at the vacuole membrane after glucose depletion (Smardon *et al.*, 2002; Smardon and Kane, 2007).

Assembly of the V_0 subcomplex occurs in the ER and requires four distinct ER-localized assembly factors (Forgac, 2007). The peripheral membrane protein Vma22p, and the integral membrane proteins Vma12p and Vma21p are dedicated to the assembly of the V_0 domain in the ER (Hirata *et al.*, 1993; Hill and Stevens, 1994; Hill and Stevens, 1995; Jackson and Stevens, 1997). In the absence of any one of these proteins, the V_0 subunits fail to assemble properly in the ER, and the V_0 subcomplex does not exit the ER (Graham *et al.*, 2003). In addition, Vma21p has been shown to escort the V-ATPase complex out of the ER, separating from the complex in a post-ER organelle and then retrieved back to the ER by cellular machinery recognizing the C-terminal dilysine motif on Vma21p (Malkus *et al.*, 2004). A fourth V-ATPase assembly factor encoded by the *PKR1* gene has been found to play a role in how efficiently the V_0 subcomplex assembles in the ER. In the absence of Pkr1p, yeast cells possess a very low level (~5–10%) of properly assembled and fully functional V-ATPase complexes that exit the ER and are found on the membrane of the vacuole (Davis-Kaplan *et al.*, 2006).

The V-ATPase assembly factors have not yet been as extensively studied as the component proteins of the V-ATPase itself. Factors that function in a subtle manner are difficult to discover because in their absence cells may not exhibit a full Vma$^-$ phenotype and are therefore not recognized by conventional phenotypic screening of mutant yeast strains. We chose instead to search for proteins that physically interact with the V_0 complex, and then examine these for their effect on assembly. Here, we report the identification and characterization of an ER-localized protein, Voa1p, that functions with Vma21p in assembly of the V-ATPase. Voa1p was identified by mass spectrometry as a component of the partially assembled V_0–Vma21p complex in the ER. Voa1p localizes to the ER due to a C-terminal dilysine motif, and it associates with Vma21p when the V_0 subcomplex is partially assembled, but not when this complex is fully assembled. Cells lacking Voa1p have slightly reduced V-ATPase activity but do not show a Vma$^-$ phenotype. An early V-ATPase assembly function for Voa1p is revealed in yeast cells expressing an ER retrieval-deficient form of the assembly factor Vma21p. In these cells, the loss of Voa1p results in a dramatic growth phenotype due to the lack of properly assembled V-ATPase.

MATERIALS AND METHODS

Plasmids and Yeast Strains

Standard protocols for molecular biology were followed (Sambrook and Russel, 2001). Plasmids used in this study are listed in Table 2. *VOA1* plus flanking sequence was amplified by polymerase chain reaction (PCR) from

Table 1. Yeast strains used in this study

Strain	Genotype	Reference
SF838-1Dα	*MATα ura3-52 leu2-3,112 his4-519 ade6 pep4-3 gal2*	Rothman and Stevens (1986)
GFY96	SF838-1Dα; *vma9Δ::Nat^r*	This study
KHY5	SF838-1Dα; *VMA21::HA*	Hill and Stevens (1994)
KHY31	SF838-1Dα; *vph1Δ::LEU2*	Graham *et al.* (1998)
LGY113	SF838-1Dα; *vma3Δ::Kan^r*	Compton *et al.* (2006)
LGY114	SF838-1Dα; *vma11Δ::Kan^r*	Compton *et al.* (2006)
LGY115	SF838-1Dα; *vma16Δ::Kan^r*	Compton *et al.* (2006)
LGY120	SF838-1Dα; *vph1Δ::Kan^r*	Davis-Kaplan *et al.* (2006)
LGY136	SF838-1Dα; *stv1Δ::Kan^r vph1Δ::Nat^r*	Davis-Kaplan *et al.* (2006)
LGY146	SF838-1Dα; *vma1Δ::Kan^r*	Davis-Kaplan *et al.* (2006)
LGY183	SF838-1Dα; *vma21QQ::HA*	This study
LGY184	SF838-1Dα; *vma6Δ::Kan^r*	This study
MRY1	SF838-1Dα; *voa1Δ::Kan^r*	This study
MRY5	SF838-1Dα; *voa1::Hyg^r vma21QQ::HA*	This study
MRY9	SF838-1Dα; *voa1::Hyg^r VMA21::HA*	This study
MRY11	SF838-1Dα; *voa1Δ::Kan^r VMA21::HA*	This study
MRY14	SF838-1Dα; *voa1::Hyg^r*	This study
TASY006	SF838-1Dα; *vma21Δ::Kan^r*	Compton *et al.* (2006)

Table 2. Plasmids used in this study

Plasmid	Description	Reference
pRS315	*CEN, LEU2*	Sikorski and Hieter (1989)
pRS316	*CEN, URA3*	Sikorski and Hieter (1989)
pGF06	pRS316 *VPH1::GFP::HIS5*	This study
pKH28	pRS316 *VMA21::HA*	Hill and Stevens (1994)
pLG271	pRS315 *VMA21::HA*	This study
pMR072	pRS316 *HA::VOA1*	This study
pMR0712	pRS316 *HA::voa1QQ*	This study
pMR0713	pRS316 *c-myc::VOA1*	This study

BY4741 (Invitrogen, Carlsbad, CA) genomic DNA. The PCR product was digested with HindIII and MscI to produce a fragment containing *VOA1* plus 821 base pairs and 245 base pairs of 5′- and 3′-flanking sequence, respectively. This fragment was inserted into HindIII and SmaI sites of pRS316 to give pMR063. A single hemagglutinin (HA) epitope tag was inserted after Asp25 of *VOA1* by using pMR063 as template by overlap extension PCR (Sambrook and Russel, 2001) with two primers having overlapping HA coding sequence at their 5′ ends, and two pRS316-specific flanking primers. The PCR product, digested with HindIII and XbaI of the pRS316 multiple cloning site, was ligated into the same sites of the same vector to give pMR072. The same technique was used to place an HA tag after the Met1 start codon of *VOA1*. A modified QuikChange protocol (Zheng *et al*., 2004) was used to introduce K262Q, K263Q mutations in pMR072 to give pMR0712. A single c-myc tag was placed after Asp25 in *VOA1* by inverse PCR (Ansaldi *et al*., 1996) by using pMR063 as template and two primers with 5′-overlapping c-myc coding sequence containing a silent BglII site. BglII-digested PCR product was ligated to produce pMR0713. All plasmids inserts prepared were confirmed by DNA sequencing. pLG271 was generated by isolating the *VMA21::HA* insert from pLG233 (pRS316 *VMA21::HA*) by digestion with SalI and Not1 and ligating into pRS315 digested with the same enzymes. pGF06 was generated by gap-repair of *VPH1::GFP::HIS5* from the genome of the appropriate strain from the Yeast GFP Clone Collection (Invitrogen) by transformation with EcoRI-digested pDJ53 (pRS316 *VPH1*) and selection on SD minus uracil and histidine.

Yeast manipulations were done in SF838–1Dα, and all strains used are listed in Table 1. To make *vma6*Δ*::Kan*^{r} (LGY184), the drug resistance marker *Kan*^{r} plus 300 base pairs of flanking sequence was amplified from cognate BY4743 strains of the homozygous diploid genome deletion collection (Open Biosystems, Huntsville, AL), propagated in pCR4Blunt-TOPO (Invitrogen), reamplified, transformed into SF838–1Dα, and selected on YEPD pH 5.0 plus G418 (Invitrogen). The fragment for *VOA1* gene replacement was amplified from the corresponding BY4741 strain of the haploid genome deletion collection and used to make *voa1*Δ*::Kan*^{r} (MRY1) by transforming the wild-type yeast strain SF838-1Dα, and *voa1*Δ*::Kan*^{r} *VMA21::HA* (MRY11) by transforming KHY5. The *vma9*Δ*::Nat*^{r} (GFY96) strain used in this study represents a replacement with *Nat*^{r} of *VMA9(YCL005W-A*) and the overlapping open reading frame (ORF) *YCL007C*. To prepare this strain, natMX4 was amplified from pAG25 (Goldstein and McCusker, 1999) by using primers with 5′ overhangs complementary to *YCL007C* flanking sequence and *VMA9(YCL005W-A*) flanking sequence. The PCR product was transformed into BY4741 *ycl007c*Δ*::Kan*^{r} to make *ycl005w-A-ycl007c*Δ*::Nat*^{r} (GFY90). This region plus 500 base pairs of flanking sequence was amplified and transformed into SF838–1Dα giving *vma9*Δ*::Nat*^{r} (GFY96). LGY183 was generated by loop in/loop out procedure by using MscI-digested pRS306 *vma21QQ::HA* (pLG76). For *VOA1* gene disruption with *Hyg*^{r}, a PCR fragment was prepared by amplification of the hphMX4 cassette from pAG32 (Goldstein and McCusker, 1999) by using a left primer having a 5′ overhang identical to 72 base pairs *VOA1* flanking sequence and a right primer with a 5′ overhang identical to 72 base pairs Voa1p N-terminal coding sequence with the first two nucleotides omitted. This fragment was transformed into SF838–1Dα, LGY183 and KHY5 to yield *voa1::Hyg*^{r} (MRY14), *voa1::Hyg*^{r} *vma21QQ::HA* (MRY5) and *voa1::Hyg*^{r} *VMA21::HA* (MRY9), respectively.

Culture Conditions

Yeast were cultured in YEPD (1% yeast extract, 2% peptone, and 2% dextrose), YEPD buffered to pH 5.0 by using 50 mM succinate/phosphate plus 0.01% adenine, or yeast nitrogen base synthetic complete minimal medium supplemented with dextrose (SD) and amino acids as needed using standard techniques. To test the growth phenotype of various yeast strains, exponentially growing yeast cells cultured in SD medium plus appropriate amino acids were diluted to cell densities measuring 1.0 OD_{600} and then further serially diluted 10-fold and spotted on agar medium. We spotted 5 μl of the starting culture and each dilution onto YEPD pH 5.0 agar, YEPD + 100 mM $CaCl_2$ agar, or YEPD pH 7.5 by using 50 mM HEPES + 50 mM $CaCl_2$ agar and incubated 48 h at 30°C. Alternatively, 2 μl of 0.8 OD_{600}/ml cultures and eightfold serial dilutions thereof were spotted.

Affinity Purification for Mass Spectrometry

*vph1*Δ (KHY31) yeast cells expressing Vma21p-HA from plasmid pKH28 and control strain *vph1*Δ without plasmid were grown in SD medium, diluted to 0.4 OD_{600}/ml in YEPD pH 5.0, and grown to OD_{600} = 1. Cells (500 OD) were collected by centrifugation and suspended on ice in phosphate-buffered saline (PBS) (126 mM NaCl, 2.5 mM KCl, and 10 mM Na_2HPO_4/KH_2PO_4, pH 7.1) plus protease inhibitors (EDTA-free 1× Complete; Roche Diagnostics, Indianapolis, IN), 2 mM benzamidine, and 1 mM phenylmethylsulfonyl fluoride). Glass bead lysates were obtained using a vortex mixer (Catley, 1988), debris and unlysed cells were removed by centrifugation (500 × *g*; 10 min; 4°C), and the pellet was washed once. The combined supernatants were centrifuged (13,000 × *g*; 20 min; 4°C), and the pellet, constituting the membrane fraction, was washed once. Membranes were solubilized by suspension in 4 ml of P13 buffer (1% $C_{12}E_9$; Sigma-Aldrich, St. Louis, MO) in PBS plus protease inhibitors) and incubated on ice for 1 h with occasional agitation. The solubilized membrane fraction was cleared by centrifugation (16,000 × *g*; 15 min; 4°C), and the supernatant was transferred to a disposable column containing 40 μl of washed anti-HA agarose (80 μl of 50% slurry, Sigma-Aldrich or Covance Research Products, Berkeley, CA). Proteins were batch adsorbed for 2 h at 4°C with gentle agitation. The affinity resin was washed at 4°C with 4 × 1 ml of P13 buffer and 0.75 ml of Tris-buffered saline (TBS) (150 mM NaCl and 50 mM Tris-HCl, pH 7.5) followed by light centrifugation (1000 × *g*; 10 s). Columns were moved to room temperature and a two-step elution (60 μl, 10 min followed by 75 μl, 20 min) was used to recover bound proteins. The elution buffer used was either 0.4 mg/ml HA peptide (Sigma-Aldrich), 0.05% $C_{12}E_9$ in TBS, or 8 M urea, 0.05% $C_{12}E_9$ in TBS. Affinity purification from *vph1*Δ (KHY31) cells with and without HA-Voa1p expressed from plasmid (pMR072) was done in the same manner, except 140 OD of cells were used, and the protocol was scaled accordingly. The elution buffer used was 0.1 M glycine-HCl, pH 2.8. Affinity extracts were separated on analytical 10–20% SDS-polyacrylamide gel electrophoresis (PAGE) minigels (Bio-Rad, Hercules, CA) and silver stained (SilverQuest; Invitrogen) for inspection, and separated on preparative gels stained with silver or Coomassie (SimplyBlue SafeStain; Invitrogen) for mass spectrometry.

Identification of Proteins by Mass Spectrometry

Sections were excised from SDS-PAGE gels, washed with water, and "in gel" protein digestion with trypsin was carried out using published protocols (Shevchenko *et al*., 1996), both with and without reduction/alkylation before the tryptic digest. Peptide samples were concentrated and desalted using microC_{18} ZipTips (Millipore, Billerica, MA) and dried. Mass spectrometry data were collected and evaluated at the Proteomics Shared Resource (Fred Hutchinson Cancer Research Center, Seattle, WA) and at the University of Oregon Proteomics Facility (Eugene, OR). The samples were resuspended and analyzed by liquid chromatography (LC)/electrospray ionization tandem mass spectrometry (MS/MS), with a two-dimensional nano-high-performance liquid chromatograph (Eksigent, Dublin, CA) coupled to a LTQ-FT (Thermo Scientific, Waltham, MA) mass spectrometer using an instrument configuration as described (Yi *et al*., 2003). In-line de-salting (5-μm, 200 Å Magic C_{18}AQ resin, Michrom Bioresources, Auburn, CA) was followed by peptide separations on a 75 μm × 250 mm Picofrit (New Objective, Woburn, MA) reversed-phase column packed with Magic 5-μm 100 Å C_{18}AQ resin (Michrom Bioresources) directly mounted on the electrospray ion source. A 400 nl/min gradient from 2 to 40% acetonitrile in 0.1% formic acid followed by 80% acetonitrile, 0.1% formic acid was used for chromatographic separations. The linear ion trap Fourier transform (FT) instrument was operated in the data-dependent mode, switching automatically between MS survey scans in the FT analyzer and MS/MS spectra acquisition in the linear ion trap. The five most intense ions from the FT full scan were selected for fragmentation. Selected ions were dynamically excluded for 45 s. Collected mass spectrometry data were subjected to the protein database search algorithm X!Tandem (Craig and Beavis, 2004) configured with the COMET score module plug-in (MacLean *et al*., 2006), and identifications were validated using PeptideProphet (Keller *et al*., 2002). The protein database used for peptide identification was the translated open reading frame FASTA file from the Saccharomyces Genome Database (www.yeastgenome.org) downloaded 1 November 2006. Peptide identification results were filtered and sorted in Computational Proteomics Analysis System (Rauch *et al*., 2006) by using a Peptide Prophet minimum probability cut-off of 0.9 and an ion% cut-off of 0.15.

Protein Extraction from Membranes

A glass-bead lysate was prepared from *voa1::Hyg*^{r} cells expressing HA-Voa1p (pMR072) as described under Affinity Purification. After removal of large particles by centrifugation, the sample was divided into thirds (22 OD equivalents each). Membrane pellets were obtained by centrifugation (13,000 × *g*; 20 min; 4°C) and washed once. Membrane protein solubilization was done essentially as published previously (Kaiser *et al*., 2002). Briefly, the pellets were suspended in 0.2 ml of either PBS or 0.1 M $NaCO_3$, pH 11.5, or 1% Triton X-100 in PBS with protease inhibitors included in all three treatments. The

suspensions were incubated on ice for 45 min and then centrifuged (100,000 × *g*; 30 min; 4°C). The supernatant fractions were removed and saved separately; the pellet fractions were reconstituted in their respective treatment conditions to the same volume as the supernatant fraction. All fractions were adjusted to contain 0.8× sample buffer (1× sample buffer: 8 M urea, 5% SDS, 5% β-meraptoethanol, 0.01% bromphenol blue, 40 mM Tris-HCl, pH 6.8) and resolved by SDS-PAGE. Western blots were prepared using the following primary antibodies: monoclonal anti-Pho8p (1D3; Invitrogen), rabbit anti-Vma6p (Bauerle *et al*., 1993), or monoclonal anti-HA (Sigma-Aldrich). Goat anti-mouse or anti-rabbit secondary antibodies conjugated to horseradish peroxidase were used (Jackson ImmunoResearch Laboratories, West Grove, PA) and detected by enhanced chemiluminescence (ECL).

Endoglycosidase H (Endo H) Assay

Solubilized membranes were prepared from *voa1*Δ*::Kan*^{r} cells expressing HA-Voa1p (pMR072) as described under Affinity Purification, except glass bead lysis was in 10 mM Na_2HPO_4/KH_2PO_4, pH 7.1, and membranes were solubilized with 1% $C_{12}E_9$ in the same buffer. Both treatments were done in the presence of protease inhibitors. A portion of the cleared, solubilized membrane fraction was withdrawn to serve as untreated control. Of the remainder, 2 OD_{600} equivalents were denatured in 0.5% SDS, 1% $C_{12}E_9$, 40 mM dithiothreitol, 3.5 mM phosphate buffer, pH 7.1, in a final volume of 40 μl and incubated at 55°C for 15 min. Then, 32 μl of 1.25% $C_{12}E_9$, 125 mM sodium citrate, pH 5.5, 2.5× protease inhibitors were added, mixed, and 36 μl was dispensed into tubes containing 4 μl of Endo H_f (New England Biolabs, Ipswich, MA) or 4 μl of Endo H_f-storage buffer (50 mM NaCl, 2 mM EDTA, and 50 mM Tris-HCl, pH 7.5). The resulting 40-μl reaction and control were incubated at 37°C for 3 h. Samples were adjusted to contain 0.8× sample buffer and analyzed by SDS-PAGE followed by immunoblotting by using monoclonal anti-HA primary antibody (Sigma-Aldrich) and horseradish conjugated anti-mouse secondary antibody (Jackson ImmunoResearch Laboratories). Blots were developed using ECL.

Whole Cell Extract Preparation and Immunoblotting

Yeast cultures were raised in SD medium, diluted to 0.4 OD_{600}/ml in YEPD, pH 5.0, and grown to OD_{600} = 1. Ten OD_{600} of cells were harvested, chilled on ice and suspended in 0.1 ml of 1× sample buffer. Ice-cold glass beads (0.1 ml) were added and the suspension vortexed 4× for 1 min with 1-min cooling intervals on ice. Lysates were removed by pipetting and cleared by centrifugation. The supernatants, constituting the whole cell extracts, were resolved by SDS-PAGE, transferred to nitrocellulose membranes, and probed with antibodies. Monoclonal primary antibodies used were anti-HA (Covance Research Products), anti-Vph1p (10D7; Invitrogen), anti-Vma1p (8B1; Invitrogen), and anti-Dpm1p (5C5; Invitrogen), with secondary horseradish-conjugated anti-mouse antibody (Jackson ImmunoResearch Laboratories), followed by ECL detection.

Native Immunoprecipitation

Analysis of c-myc-Voa1p coimmunoprecipitation with Vma21p-HA was done following the Affinity Purification for Mass Spectrometry protocol with the following modifications: 100 OD_{600} of cells were used, and the protocol was scaled proportionally. A portion of the cleared, solubilized membrane fraction was adjusted to 0.8× sample buffer to serve as measure of protein input, the remainder was adsorbed to 10 μl of anti-HA agarose (Sigma-Aldrich). The resin was washed, and bound proteins were recovered by elution with 2× 30 μl of 1× sample buffer but omitting β-meraptoethanol and bromphenol blue. Input and immunoprecipitates were separated on SDS-PAGE gels and analyzed by Western blotting by using monoclonal anti-Vph1 (10D7) and polyclonal anti-c-myc (Santa Cruz Biotechnology, Santa Cruz, CA) primary antibodies. Equal amounts of Vma21p-HA were present in input fractions well as immunoprecipitate fractions from all strains tested as ascertained by probing blots with anti-HA antibodies.

Fluorescence Microscopy

The acidification of vacuoles in various yeast strains was visualized using the lysosomotropic fluorescent dye quinacrine. Quinacrine staining of live yeast cells was conducted as described previously (Weisman *et al*., 1987; Flannery *et al*., 2004). Quinacrine was used at a final concentration of 200 μM prepared in 100 mM 2-(*N*-morpholino)ethanesulfonic acid (MES), pH 7.7, to stain acidified vacuoles, whereas concanavalin A tetramethylrhodamine (Invitrogen) was added at a final concentration of 50 μg/ml to allow for fluorescent visualization of the cell surface.

Localization of green fluorescent protein (GFP)-tagged proteins and stained DNA were determined by fluorescence microscopy. One milliliter of exponentially growing cells was harvested by centrifugation for 30 s and resuspended in 100 mM MES, pH 7.7, 2% glucose, and 5 mg/ml Hoechst 33342 DNA dye. Cells were fixed by the addition of formaldehyde solution (final concentration, 3.7%) and incubated at room temperature for 5 min. Cells were collected by centrifugation and washed twice with buffered glucose before visualization.

Samples for indirect immunofluorescence were prepared as described previously and probed with anti-HA antibody (Covance Research Products; Conibear and Stevens, 2002). Images were acquired on an Axioplan 2 fluorescence microscope (Carl Zeiss,) using 100× objective and manipulated using AxioVision software (Carl Zeiss, Thornwood, NY).

V-ATPase Activity Assay

Yeast vacuoles were isolated from wild-type (KHY5) and *voa1::Hyg*^{r} (MRY9) strains using the method described by Uchida *et al*. (1985). Freshly prepared vacuoles were assayed for concanamycin A-sensitive ATPase activity by using a coupled spectrophotometric assay as described previously (Conibear and Stevens, 2002). Vacuole membranes prepared from wild-type and voa1::Hyg^r cells and were assayed 11 and 12 times, respectively, with the error expressed as SD.

RESULTS

Voa1p Interacts Directly with the V_0–Vma21p Complex

Previous work has shown that the V-ATPase V_0 subunits assemble in the ER and bind directly to the assembly factor Vma21p (Malkus *et al*., 2004). It was noted that in addition to the known V_0 subunits, there are other proteins present in this assembly complex that have not yet been identified (Malkus *et al*., 2004). We chose mass spectrometry as a tool to examine the V_0–Vma21p complex for uncharacterized members in the early stage of assembly in the ER membrane. A *vph1*Δ strain background was chosen because partially assembled V_0–Vma21p complex forms in the ER, but it is unable to exit the ER. HA-epitope–tagged Vma21p (Vma21p-HA) was expressed in *vph1*Δ cells and purified from solubilized membranes by affinity chromatography using gentle detergent conditions to preserve protein–protein interactions. Affinity extracts were separated by analytical SDS-PAGE and visualized by silver staining (Figure 1A). In addition to known V_0 proteins a prominent band migrated at ~35 kDa, just ahead of Vma6p. Gel sections were cut from identical preparative-scale gels and subjected to digestion with trypsin. The peptides were extracted from the gel and analyzed by LC MS/MS. The mass spectrometric results confirmed the presence of V_0 subunits but also identified the prominent unknown protein as the uncharacterized ORF YGR106C, which is predicted to encode a 265-amino acid protein (Figure 1B).

We have named this gene *VOA1* for V_0 *a*ssembly protein. Voa1p is predicted to possess two transmembrane segments, located near the N and the C terminus of the protein, respectively. The N-terminal transmembrane segment is part of a predicted signal sequence with an expected cleavage site between Ala24 and Asp25. To track Voa1p by Western blotting, a single HA-epitope tag was placed either after Met1 or Asp25 of Voa1p. Whereas Voa1p tagged after Met1 could not be detected by immunoblotting, Voa1p tagged after Asp25 was readily visible (unpublished data). This result suggests that the Voa1p signal sequence may be cleaved.

Mass spectrometric analysis of Voa1p having an HA-tag after Asp25 confirmed cleavage of the signal sequence. HA-Voa1p was expressed in *vph1*Δ cells, affinity purified, and resolved by SDS-PAGE. A section containing the appropriate band was cut from the gel, treated with trypsin, and the resulting peptides were recovered. Two signature peptides were detected by LC MS/MS; the first is as expected from the amino acid sequence of the full-length protein, but the second is formed only when Voa1p has Asp25 at its N terminus as a result of signal peptide cleavage (Figure 1C). Consequently, signal sequence cleavage produces a processed protein where the bulk of Voa1p is located on the lumenal side of the ER and the C-terminal transmembrane segment serves as an anchor (Figure 1D). This topology results in the cytosolic exposure of the C-terminal, dilysine

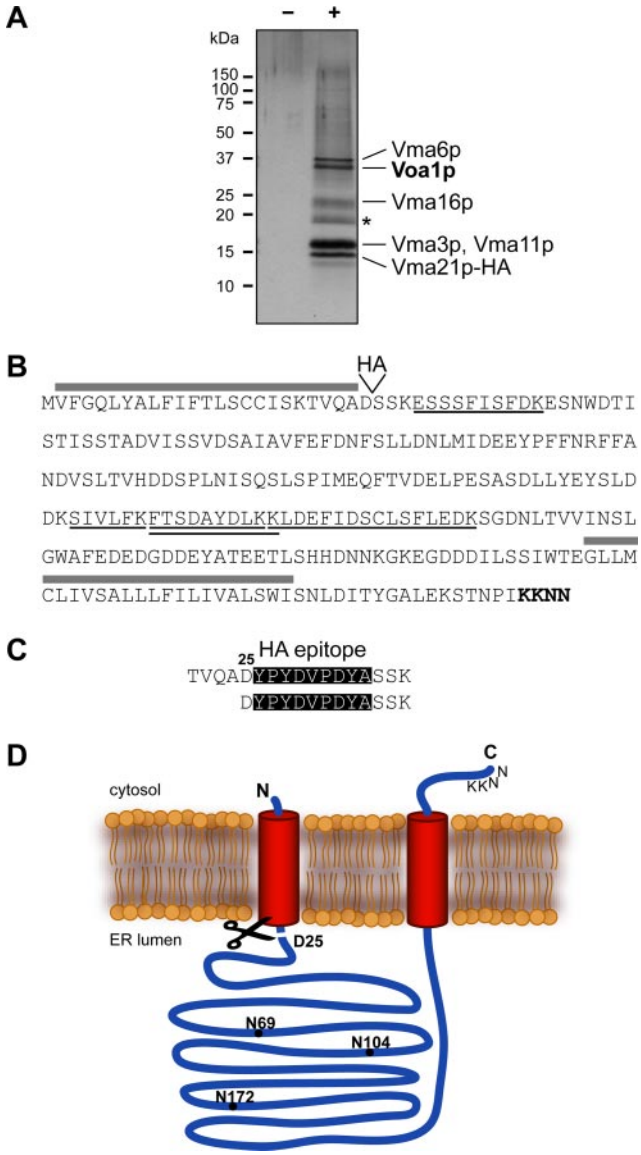

Figure 1. Voa1p associates with the V_0–Vma21p complex. (A) Voa1p copurifies with the Vma21p–HA bait protein. Detergent-solubilized membranes were prepared from *vph1*Δ (KHY31) in the absence (−) or in the presence (+) of Vma21p-HA expressed from pKH28. Vma21p-HA and copurifying proteins were captured using anti-HA agarose and then eluted and analyzed by SDS-PAGE and silver staining. Protein identifications were made by LC MS/MS using gel sections cut from identical gels but at a preparative scale. V-ATPase subunit bands were assigned based on previously observed apparent molecular mass and identification by mass spectrometry in the appropriate gel section. An unidentified protein band is marked with an asterisk. (B) Amino acid sequence of Voa1p. The position of the subsequently introduced HA epitope tag (YPYDVPDYA) is indicated. Tryptic peptides identified by mass spectrometry for the untagged protein are underlined. Gray bars indicate predicted transmembrane segments (SOSUI; Hirokawa *et al.*, 1998). The predicted ER retrieval motif (KKXX) at the C terminus is shown in bold. (C) Two peptides generated by digestion of HA-tagged Voa1p with trypsin allow the detection of N-terminal signal sequence cleavage. Placement of the HA-tag (black background) adjacent to the predicted signal cleavage site between Ala-24 and Asp-25 (SignalP; Bendtsen *et al.*, 2004) results in the two possible tryptic peptides shown, depending on whether signal cleavage occurs. (D) Topology model of Voa1p. The model shows cleavage of the 24-amino acid signal sequence (scissors), leaving Asp25 at the newly formed N terminus. The bulk of Voa1p is exposed to the lumenal side of the ER and consists of a predicted globular domain anchored to the ER membrane by a transmembrane segment near the C terminus of the protein. The three possible sites for N-glycosylation are indicated (N69, N104, and N172). The C terminus contains an ER retention and retrieval signal (KKNN) facing the cytosol.

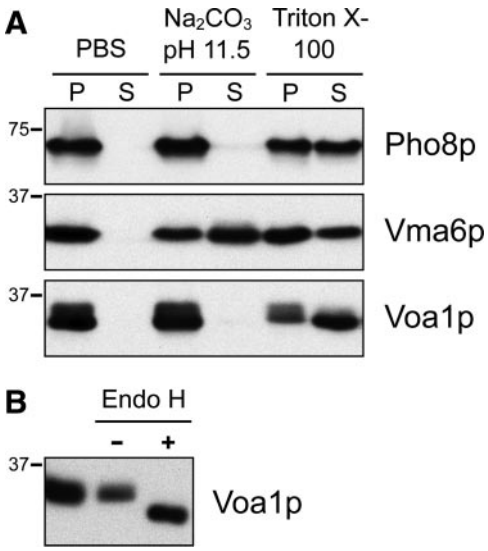

Figure 2. Voa1p is a glycosylated, integral membrane protein. (A) Membrane proteins prepared from *voa1::Hyg*^{r} (MRY14) cells expressing HA-Voa1p (pMR072) were divided into equal aliquots and treated with buffer only (PBS), 100 mM Na_2CO_3, pH 11.5, or with 1% Triton X-100. After centrifugation at 100,000 × *g* for 30 min, the pellet (P) and supernatant (S) fractions were analyzed by SDS-PAGE followed by Western blotting using antibodies against Pho8p (integral membrane protein), Vma6p (peripheral membrane protein), and HA to detect HA-Voa1p. Gels contained equal amounts of protein per lane. (B) Membrane proteins prepared from *voa1*Δ*::Kan*^{r} cells (MRY1) expressing HA-Voa1p (pMR072) were solubilized [left lane] and then incubated for 3 h with (+) or without (−) Endo H. Samples were analyzed by SDS-PAGE and Western blotting using anti-HA antibodies to detect HA-Voa1p. The molecular mass (kilodaltons) of the nearest marker protein is given on the left.

ER retention motif, KKNN, and would make available three asparagine residues in the lumenal domain as sites of possible N-linked glycosylation (Figure 1D).

Voa1p Is an Integral Membrane Glycoprotein

To confirm that Voa1p is an integral membrane protein, membrane fractions were prepared from yeast cells expressing HA-Voa1p and treated with either PBS, Na_2CO_3, pH 11.5, or 1% Triton X-100. Alkali treatment with Na_2CO_3 extracts peripherally associated membrane proteins from isolated membranes but not integral membrane proteins, which can only be extracted by solubilization with detergent (Fujiki *et al.*, 1982). The integral membrane protein alkaline phosphatase (Pho8p) and the V-ATPase peripheral membrane protein Vma6p served as controls. As shown in Figure 2A, the integral membrane protein control Pho8p remained in the membrane pellet fraction (P) after treatment with either buffer or Na_2CO_3. Treatment with the detergent Triton X-100 was required to produce soluble Pho8p that can be extracted into the supernatant fraction (S). The peripheral membrane protein control Vma6p was extracted from the membrane pellet fraction into the supernatant fraction by

treatment with either Na_2CO_3 or detergent. Like Pho8p, Voa1p remained with the membrane pellet fraction when treated with buffer or Na_2CO_3 and was only extracted from the membranes by treatment with detergent, indicating that Voa1p is an integral membrane protein.

HA-Voa1p migrates on SDS-PAGE gels with an apparent molecular mass of ~36 kDa, as shown in Figure 2A, bottom. This is larger than both the 30.8 kDa predicted for the full-length protein and the 28.1-kDa protein resulting from signal cleavage. Carbohydrate addition to one or more of the three *N*-glycosylation sites present in Voa1p could contribute to this increase in apparent molecular mass (Figure 1D). To examine this, solubilized membranes prepared from cells expressing HA-Voa1p were denatured with SDS at 56°C for 15 min, followed by incubation with Endo H at 37°C for 3 h, and HA-Voa1p analyzed by Western blotting. The results in Figure 2B show that Voa1p in the sample treated with Endo H migrated as a smaller protein compared with protein in the untreated sample. Denaturation under harsher conditions (65°C, 15 min or 100°C, 5 min) and extending the Endo H digest (37°C, 18 h) gave the same results. The apparent size difference of ~2 kDa is consistent with oligosaccharide addition to a single asparagine residue (Kaiser *et al.*, 2002). These results confirm that Voa1p is modified by glycosylation of at least one site present in the lumenal domain of the protein.

Voa1p Is Required for V_0 Assembly in vma21QQ Cells

Voa1p and Vma21p are encoded by neighboring ORFs on chromosome VII, and the two proteins are encoded on opposite strands, separated by only 156 base pairs of 3′-noncoding sequence (Figure 3A). Western blots of extracts from a *voa1*Δ*::Kan*^{r} strain with an integrated HA-tagged *VMA21* allele (*VMA21::HA*) revealed that Vma21p levels were reduced two- to threefold in the *voa1*Δ*::Kan*^{r} strain relative to wild-type cells (Figure 3B), with Dpm1p (an unrelated ER membrane protein) as a loading control. Furthermore, introducing plasmid-expressed Voa1p into *voa1*Δ*::Kan*^{r} cells did not return Vma21p levels to those found in wild-type cells. Thus, replacing the *VOA1* ORF with *Kan*^{r} interfered with the expression level of Vma21p. A second *voa1* null mutant was prepared where the *VOA1* coding sequence was disrupted by replacing the first two nucleotides of the start codon with *Hyg*^{r}. This leaves intact 952 nucleotides of *VMA21* 3′-flanking sequence (Figure 3A), and in this strain Vma21p levels were indistinguishable from wild-type cells (Figure 3B). All subsequent experiments characterizing the loss of Voa1p were carried out using the insertional disruption of *VOA1* by *Hyg*^{r} (*voa1::Hyg*^{r}).

Yeast cells lacking a functional V-ATPase are unable to grow on rich media buffered to neutral pH and containing elevated $CaCl_2$; yet, they are able to grow on rich media buffered to an acidic pH of 5.0 (Kane, 2006). The growth phenotype of cells lacking Voa1p was compared with wild-type yeast cells and with cells lacking the V-ATPase assembly factor Vma21p. As shown in Figure 4A, wild-type cells grew on media buffered to pH 5.0 as well as $CaCl_2$ media

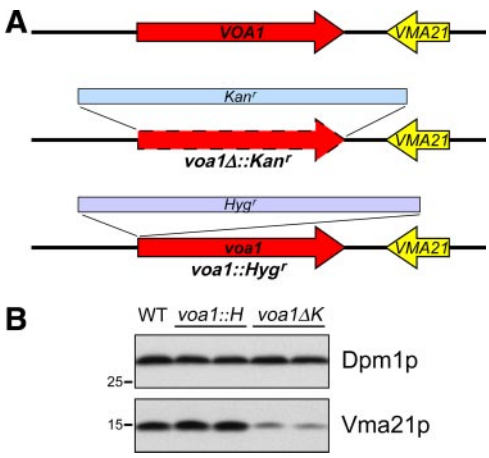

Figure 3. Disruption of Voa1p by insertional mutagenesis does not affect protein levels of Vma21p. (A) Schematic of the genomic location of *VOA1* and *VMA21*. The two ORFs are separated by 156 base pairs. Deletion of the *VOA1* ORF by replacement with the kanMX4 cassette (*Kan*^{r}) generating *voa1*Δ*::Kan*^{r} (MRY1) is outlined, in addition to the construction of the *voa1::Hyg*^{r} (MRY14) allele, wherein the *VOA1* ORF is disrupted by insertion of the hphMX4 cassette (*Hyg*^{r}) with concomitant deletion of the first two nucleotides of the *VOA1* start codon. The *voa1::Hyg*^{r} allele maintains 952 nucleotides of native *VMA21* 3′ sequence. (B) Western blot analysis of whole cell extracts from yeast strains each of which has an integrated *VMA21::HA* allele; wild-type *VOA1* (WT; KHY5), *voa1::Hyg*^{r} (*voa1::H*; MRY9), and *voa1*Δ*::Kan*^{r} (*voa1*Δ*K*; MRY11). Blots were probed with anti-HA antibodies to detect Vma21p-HA and antibodies against Dpm1p as a loading control. Protein samples in lanes 2 and 3 and 4 and 5 are prepared from two independent isolates. The molecular mass (kilodaltons) of the nearest marker protein is shown on the left.

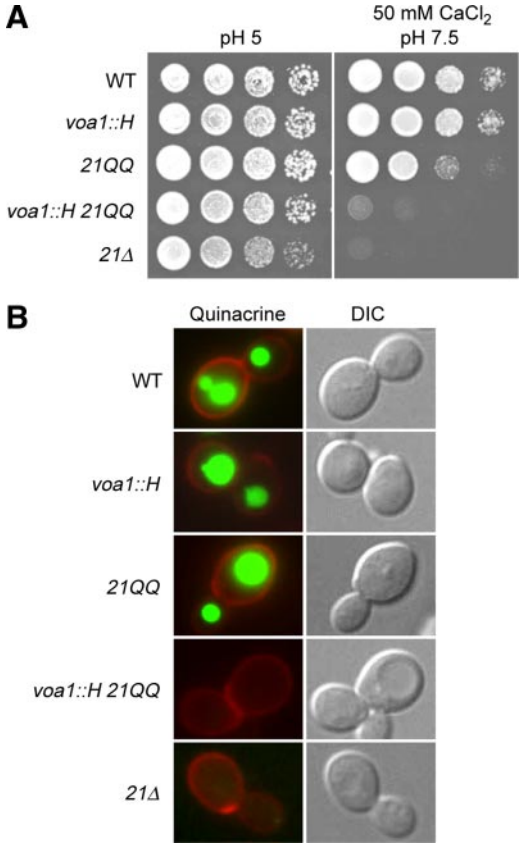

Figure 4. Loss of Voa1p in cells expressing Vma21pQQ results in calcium sensitivity and lack of vacuolar acidification. (A) Exponentially growing cultures of wild-type (WT; SF838–1Dα), *voa1::Hyg*^{r} (*voa1::H*; MRY14), *vma21QQ* (*21QQ*; LGY183), *voa1::Hyg*^{r} *vma21QQ* (*voa1::H 21QQ*; MRY5), and *vma21*Δ (*21*Δ; TASY006) were serially diluted and spotted onto rich media buffered to pH 5.0 or rich media buffered to pH 7.5 plus 50 mM $CaCl_2$. (B) The same strains were stained with quinacrine (green) and concanavalin A-tetramethylrhodamine (red) and viewed by either fluorescent or DIC microscopy.

buffered to pH 7.5. As expected, yeast cells lacking the assembly factor Vma21p failed to grow in the presence of elevated $CaCl_2$, due to disruption of V-ATPase function. Yeast cells lacking Voa1p exhibited near wild-type growth even in the presence of elevated $CaCl_2$. However, it is possible that the loss of Voa1p reduces V-ATPase function, but the reduction may not be severe enough to affect growth in the presence of elevated $CaCl_2$. V-ATPase activities were measured for vacuoles from WT and *voa1::Hyg*^{r} cells, and *voa1::Hyg*^{r} vacuoles have slightly reduced V-ATPase activity (75 ± 14%) compared with wild-type vacuoles (100%). This level of V-ATPase activity reduction is not expected to affect growth in the presence of elevated $CaCl_2$. As has been reported, a drastic reduction in V-ATPase activity (to <25% wild-type activity) is required to observe a growth defect in the presence of elevated $CaCl_2$ (Liu and Kane, 1996; Curtis and Kane, 2002).

To further test for a role for Voa1p in V-ATPase function, we disrupted *VOA1* in cells expressing a mutated form of Vma21p, Vma21pQQ, where the dilysine motif was changed to diglutamine (QQ). The dilysine motif in Vma21p functions as an ER retention motif, because upon mutation to QQ Vma21p was no longer localized to the membranes of the ER but was found on the membrane of the vacuole (Hill and Stevens, 1994; Malkus *et al*., 2004). Vma21pQQ is partially functional as a V-ATPase assembly factor, because vacuoles isolated from *vma21QQ* cells had ~30% of wild-type V-ATPase activity (Hill and Stevens, 1994). Yeast cells expressing Vma21pQQ exhibited wild-type growth on rich media buffered to pH 5.0, but they displayed slightly compromised growth on buffered $CaCl_2$ media (Figure 4A). An even more dramatic growth defect was observed when cells expressing Vma21pQQ also lacked Voa1p. As shown in Figure 4A, *voa1::Hyg*^{r} *vma21QQ* double mutant cells grew well on rich media buffered to pH 5.0, but they were unable to grow on buffered $CaCl_2$ media. The growth phenotype of *voa1::Hyg*^{r} *vma21QQ* yeast on buffered $CaCl_2$ was similar to *vma21*Δ cells, which completely lack a functional V-ATPase. These results indicate that loss of Voa1p has an effect on V-ATPase activity, and this effect is more dramatic in the sensitized background of cells expressing an ER retrieval-deficient form of Vma21p.

Because the function of the V-ATPase is to bring about acidification of the vacuole in yeast, we tested for a defect in vacuolar acidification in *voa1::Hyg*^{r} *vma21QQ* yeast cells. Quinacrine is a fluorescent dye that accumulates in acidic cellular compartments (Uchida *et al*., 1985; Conibear and Stevens, 2002). After quinacrine uptake, wild-type cells exhibited highly fluorescent vacuoles that showed up as bright green disks when visualized by microscopy (Figure 4B). The binding of concanavalin A-tetramethylrhodamine isothiocyanate to the yeast cell wall showed the outline of the yeast cells in red. Yeast cells expressing Vma21pQQ also accumulate quinacrine, demonstrating vacuolar acidification even though these cells have reduced levels of V-ATPase on the vacuolar membrane. Similarly, *voa1::Hyg*^{r} cells accumulate quinacrine in their vacuoles. Cells lacking Voa1p and expressing Vma21pQQ (*voa1::Hyg*^{r} *vma21QQ*) failed to accumulate quinacrine, similar to cells completely lacking V-ATPase function (*vma21*Δ cells). This result indicates that *voa1::Hyg*^{r} *vma21QQ* yeast cells lack a functional V-ATPase on their vacuolar membranes and are unable to acidify their vacuoles.

Loss of Voa1p Enhances the V-ATPase Assembly Defect of vma21QQ Cells

The demonstrated loss of V-ATPase function in cells lacking Voa1p and expressing Vma21pQQ could be a result of either a nonfunctional V-ATPase on the vacuole or reduced levels of V-ATPase on the vacuole due to an assembly defect. The V_0 subunit Vph1p is normally a very stable protein if upon synthesis it is assembled into the V_0 subcomplex and transported to the vacuole membrane (Graham *et al*., 2003). However, the levels of Vph1p are dramatically reduced in cells that are defective in the assembly of a complete V_0 subcomplex, which is the case when individual V_0 subunits or assembly factors (Vma21p, Vma12p, Vma22p, or Pkr1p) are absent (Graham *et al*., 2003; Compton *et al*., 2006; Davis-Kaplan *et al*., 2006). To test for defective V_0 assembly, cell extracts were prepared and analyzed by Western blotting for the presence of Vph1p, the V_1 protein Vma1p, and Dpm1p as a loading control. As expected, we found that cellular levels of Vma1p present at steady-state are similar in all strains tested; wild-type, the single mutants *vma21QQ* and *voa1::Hyg*^{r}, the double mutant *voa1::Hyg*^{r} *vma21QQ*, and *vma21*Δ (Figure 5). Because the V_1 subcomplex can assemble independently of the V_0 subcomplex (Doherty and Kane, 1993; Graham *et al*., 2003), V_1 protein levels are generally unaffected by any defect in V_0. Consistent with near wild-type growth and quinacrine accumulation for the single mutants *vma21QQ* and *voa1::Hyg*^{r}, Vph1p levels in these strains were similar to that of wild-type cells (Figure 5). Likewise, a Western blot of more dilute extracts from wild-type and *voa1::Hyg*^{r} cells failed to reveal differences in Vph1p levels between these cells types (unpublished data). In contrast, the levels of Vph1p were clearly reduced in *voa1::Hyg*^{r} *vma21QQ* yeast cells compared with wild-type cells, and they were more similar to Vph1p levels found in *vma21*Δ cells, which have no detectable functional V-ATPase on the vacuole.

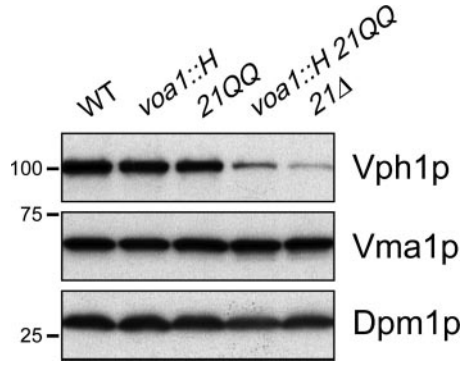

Figure 5. Loss of Voa1p in cells expressing Vma21pQQ results in reduced levels of V_0 subunit Vph1p. Whole cell extracts were prepared from wild type (WT) (KHY5), *voa1::Hyg*^{r} (*voa1::H*; MRY9), *vma21QQ* (*21QQ*; LGY183), *voa1::Hyg*^{r} *vma21QQ* (*voa1::H 21QQ*; MRY5), and *vma21*Δ (*21*Δ; TASY006). Proteins were separated by SDS-PAGE and probed with anti-Vph1p and anti-Vma1p antibodies. Anti-Dpm1p antibody was included as a loading control. The molecular mass (kilodaltons) of the nearest marker protein is shown on the left.

We next tested whether the Vph1p present in *voa1::Hyg*^{r} *vma21QQ* yeast cells represents a small amount of fully assembled complex on the vacuole membrane or protein trapped in the ER due to a V_0 assembly defect. To address this question, we introduced GFP-tagged Vph1p expressed from a low-copy plasmid into wild-type, *vma21*Δ, and *voa1::Hyg*^{r} *vma21QQ* yeast cells, and we visualized Vph1p localization by using fluorescence microscopy. In wild-type cells Vph1p-GFP was assembled into the V-ATPase and targeted to the membrane of the vacuole as observed by GFP green fluorescent staining coincident with the outline of the

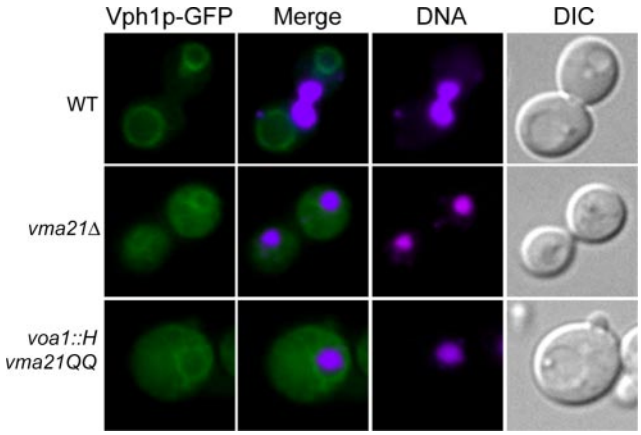

Figure 6. Vph1p fails to exit the ER in *voa1::Hyg*^{r} *vma21QQ* cells. Wild-type (WT; SF838–1Dα), *vma21*Δ (TASY006), and *voa1::Hyg*^{r} (*voa1::H*) *vma21QQ* (MRY5) cells expressing Vph1p-GFP (pGF06) were treated with the DNA binding dye Hoechst 33342 (shown as magenta) and visualized by fluorescent or DIC microscopy. Merged images show localization of Vph1p-GFP (green) to either the ER perinuclear and cortical membranes (*vma21*Δ and *voa1::H vma21QQ*) or the vacuole (WT).

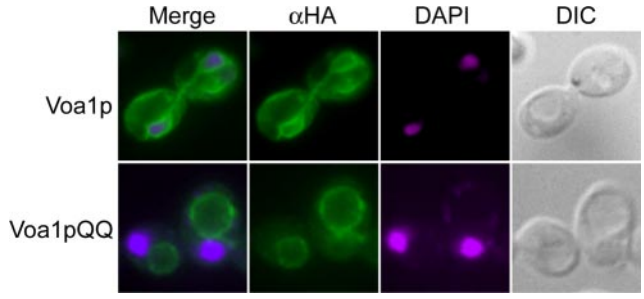

Figure 7. Voa1p requires its C-terminal dilysine motif for localization to the ER. Indirect immunofluorescence was performed on *voa1::Hyg*^{r} (MRY14) cells expressing either HA-Voa1p (pMR072) or HA-Voa1pQQ (pMR0712). Voa1p and Voa1pQQ were visualized using anti-HA antibodies, followed by goat anti-mouse biotin conjugated antibody treatment, and a streptavidin-fluorescein isothiocyanate treatment. DNA was visualized by labeling with DAPI and shown as magenta. Vacuoles were visualized by DIC microscopy. Merged images show localization of Voa1p or Voa1pQQ (green) to either the ER perinuclear and cortical membranes (HA-Voa1p) or the vacuole (HA-Voa1pQQ).

vacuole as seen by differential interference contrast (Figure 6, top). The nucleus was visualized using the DNA binding dye Hoechst 33342 and shown as a magenta dot within the cell next to the vacuole as can be seen in wild-type cells expressing Vph1p-GFP. The same localization of Vph1p-GFP on the vacuolar membrane was observed in the single mutants *vma21QQ* and *voa1::Hyg*^{r} (unpublished data).

In cells lacking the assembly factor Vma21p, Vph1p-GFP exhibited typical ER membrane staining (perinuclear in addition to staining cortical ER membranes adjacent to the plasma membrane) due to the inability of Vph1p-GFP to assemble into the V_0 subcomplex and failure to exit the ER in *vma21*Δ cells (Figure 6, middle). Vph1p-GFP in *voa1::Hyg*^{r} *vma21QQ* yeast cells also demonstrated perinuclear and cortical ER staining, rather than vacuolar staining, indicating that Vph1p was unable to exit the ER. The effect of loss of Voa1p seemed specific for the V-ATPase because a plasma membrane (Pma1p) and several vacuolar membrane proteins (Pmc1p, Zrc1p, and Pho8p) all localized normally in cells lacking Voa1p (unpublished data). Together, our results indicate that *vma21QQ* cells are dependent on Voa1p for V_0 subcomplex assembly and that Voa1p functions with Vma21p in V_0 assembly.

Voa1p Is a V-ATPase Assembly Factor Localized to the ER with Vma21p

The subcellular localization of Voa1p was determined by indirect immunofluorescence by using the HA epitope-tagged version of the protein (HA-Voa1p). Immunolocalization of HA-Voa1p revealed a perinuclear (the nucleus visualized by 4′,6-diamidino-2-phenylindole [DAPI]) and cortical ER membrane staining pattern, indicating that Voa1p localizes to the ER membrane (Figure 7). Voa1p, like Vma21p, possesses a C-terminal dilysine motif that may function in the retention of Voa1p in the ER. To test this, we examined by indirect immunofluorescence the localization of HA-Voa1p and Voa1p in which the dilysines have been changed to diglutamines (HA-Voa1pQQ). As shown in Figure 7, modification of the two amino acids in Voa1p changed the localization pattern from ER to vacuole membrane. These results indicate that Voa1p is an ER localized V-ATPase assembly factor possessing a functional dilysine ER-retrieval motif.

As mentioned, Vma21pQQ does function as a V_0 assembly factor, albeit less efficiently, even though it is mislocalized to the membranes of the vacuole. Yeast cells expressing Vma21pQQ have less V-ATPase on the vacuole due to the inability of Vma21pQQ to be retained in the ER and carry out multiple rounds of V-ATPase assembly. Like Vma21pQQ, Voa1pQQ was mislocalized to vacuole membranes. To assess how well the mislocalized Voa1pQQ functions as an assembly factor, we investigated whether Voa1pQQ could function together with Vma21pQQ in V_0 assembly. Cells lacking Voa1p (*voa1::Hyg*^{r}) and expressing Vma21pQQ (*voa1::Hyg*^{r} *vma21QQ*) were transformed with a low copy plasmid expressing either wild-type Voa1p or Voa1pQQ, and the cells were tested for their ability to grow in the presence of elevated $CaCl_2$. The *voa1::Hyg*^{r} *vma21QQ* cells expressing Voa1p grew in the presence of elevated $CaCl_2$ just as well as *vma21QQ* cells, indicating that the plasmid-borne *VOA1* gene is fully functional (Figure 8, rows 1 and 3). Surprisingly, *voa1::Hyg*^{r} *vma21QQ* cells expressing Voa1pQQ are just as sensitive to Ca^{2+} as *voa1::Hyg*^{r} *vma21QQ* cells alone (Figure 8, rows 2 and 4). Expressing Voa1pQQ from a high copy plasmid did not alleviate *voa1::Hyg*^{r} *vma21QQ* cells sensitivity to $CaCl_2$ (unpublished data). Because we found that Voa1pQQ is expressed and

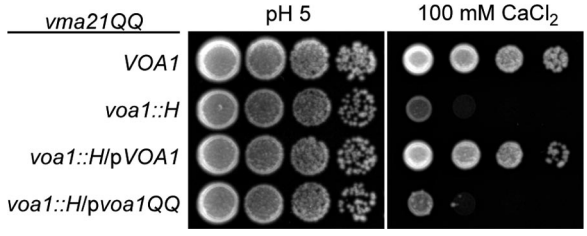

Figure 8. Retrieval deficient Voa1pQQ does not function as a V-ATPase assembly factor. Exponentially growing cultures of *vma21QQ* (LGY183), *voa1::Hyg*^{r} *(voa1::H) vma21QQ* (MRY5), and *voa1::Hyg*^{r} *vma21QQ* expressing either Voa1p (p*VOA1*; pMR072) or Voa1pQQ (p*voa1QQ*; pMR0712) were serially diluted and spotted onto rich media buffered to pH 5.0 or rich media plus 100 mM $CaCl_2$.

stable in yeast cells, our results demonstrate that mislocalization of Voa1p to the vacuole membrane completely prevents it from functioning in V_0 assembly.

Voa1p Binds to the Assembling V-ATPase Complex in the ER

Our earlier results (Figure 1A) indicated that significant amounts of Voa1p copurified with the incompletely assembled V_0–Vma21p subcomplex in *vph1*Δ cells. To better understand how Voa1p participates in the assembly of the V-ATPase, we examined in more detail the interaction of Voa1p with Vma21p. We compared the Voa1p–Vma21p interaction in various mutant backgrounds lacking individual V_0 subunits or a V_1 subunit. Vma21p-HA was immunoprecipitated under native conditions by using solubilized membrane fractions prepared from wild-type, *vma1*Δ, *vph1*Δ, *vma3*Δ, *vma6*Δ, *vma9*Δ, *vma11*Δ, and *vma16*Δ yeast cells expressing both Vma21pHA and c-myc-Voa1p.

Immunoprecipitates obtained from wild-type, *vph1*Δ, and *vma1*Δ cells were probed for the presence of Voa1p and the V_0 subunit Vph1p. As shown in Figure 9A, very little Voa1p was found associated with Vma21p in wild-type cells. At the same time significant amounts of Vph1p copurified with Vma21p from these cells (Figure 9A, top), indicating that V_0–Vma21p subcomplexes were present in wild-type cells but that they did not contain Voa1p. A similar result was observed for V_0–Vma21p subcomplexes immunoprecipitated from *vma1*Δ cells. Cells lacking the V_1 protein Vma1p assemble a complete V_0–Vma21p subcomplex that exits the ER normally, even though these cells do not form a V_1 complex and therefore have no functional V-ATPase (Graham *et al*., 2003).

In *vph1*Δ cells, we found considerable amounts of Voa1p coprecipitating with Vma21p (Figure 9A), consistent with the affinity purification results shown in Figure 1A. This result indicates that Voa1p preferentially associates with a V_0–Vma21p complex lacking Vph1p compared with the fully assembled V_0 subcomplex found in wild-type and *vma1*Δ cells.

We also examined how the loss of any of the remaining five V_0 subunits affects the interaction between Voa1p and Vma21p. In the absence of either the peripheral membrane subunit Vma6p or the integral membrane subunit Vma9p, Voa1p is found associated with the V_0–Vma21p complex (Figure 9B). As we have reported previously, *vma6*Δ or *vma9*Δ strains contain Vma3p, Vma11p, and Vma16p in incomplete V_0 subcomplexes associated with Vma21p (Malkus *et al*., 2004; Compton *et al*., 2006). These incomplete V_0 complexes remain in the ER. In addition, a small amount of Voa1p can associate with the incomplete V_0–Vma21p complex lacking Vma16p.

Vma3p, Vma11p, and Vma16p are modeled to form a "proteolipid" ring that bridges the interaction between Vma21p and the remaining V_0 subunits (Malkus *et al*., 2004; Compton *et al*., 2006; Wang *et al*., 2007). Not surprisingly, very little Voa1p immunoprecipitated with Vma21p in *vma3*Δ or *vma11*Δ cells. Vma21p and all three of the proteolipid subunits (Vma3p, Vma11p, and Vma16p) are required to form a stable proteolipid ring, and Voa1p preferentially associates with this complex. Together, our results reveal that Voa1p associates with an incompletely assembled V_0–Vma21p complex in the ER; specifically, Voa1p binds to V_0–Vma21p complexes lacking Vph1p, Vma6p, or Vma9p but containing a partially formed or preferably, a completely formed proteolipid ring.

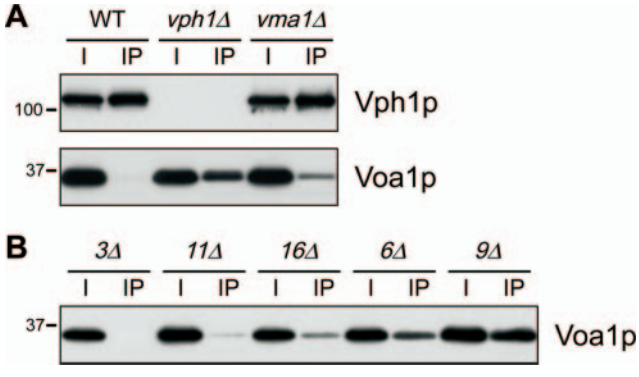

Figure 9. Voa1p associates with the assembling V_0 complex in the ER. Solubilized membranes were prepared from various *vma*Δ strains expressing both Vma21p-HA (pLG271) and c-myc-Voa1p (pMR0713), followed by immunoprecipitation of Vma21p-HA with anti-HA antibody. Proteins of the solubilized membrane input (I) and immunoprecipitate (IP) were separated by SDS-PAGE and used to generate Western blots. (A) Strains used were wild-type (WT; SF838-1Dα), *vph1*Δ (LGY120) and *vma1*Δ (LGY146), and Western blots were probed with antibodies recognizing either Vph1p or c-myc-Voa1p. (B) Strains used were *vma3*Δ (LGY113), *vma11*Δ (LGY114), *vma16*Δ (LGY115), *vma6*Δ (LGY184) and *vma9*Δ (GFY96), and Western blots were probed with antibodies recognizing c-myc-Voa1p. The molecular mass (kilodaltons) of the nearest marker protein is shown on the left.

DISCUSSION

Voa1p Functions Early in V_0 Domain Assembly

With 14 different integral and peripheral membrane subunits, some of them present in multiple copies, the V-ATPase is a complex enzyme, requiring additional protein factors for its assembly and function. Factors have been identified for the stable assembly and glucose-regulated reassembly of the V_1 and V_0 domains (Kane, 2006; Forgac, 2007). Previous work in yeast has identified four ER-localized proteins (Vma12p, Vma21p, Vma22p, and Pkr1p) that are required for the assembly of the V_0 domain of the V-ATPase (Forgac, 2007), and one of these proteins (Vma21p) escorts the V_0 domain out of the ER (Malkus *et al*., 2004). In this report, we identify a fifth V_0 assembly factor, Voa1p.

Voa1p is an ER-localized integral membrane glycoprotein, which when deleted reduces V-ATPase activity to 75% wild type but results in no apparent Vma^- phenotype, i.e., no calcium-sensitive growth and normal acidification of the vacuole. Because it takes at least a three- to fivefold reduction in the level of V-ATPase to observe increased sensitivity to Ca^{2+} in yeast cells (Liu *et al*., 1996; Curtis and Kane, 2002), the effect on the level of the V-ATPase due to loss of Voa1p is not sufficiently strong to confer a Vma^- growth phenotype. This might explain why a clear role for Voa1p in V_0 assembly was revealed in cells expressing an ER retrieval-deficient form of Vma21p (Vma21pQQ). *vma21QQ* yeast cells have reduced V-ATPase levels (Hill and Stevens, 1994) and a very mild growth defect in the presence of elevated Ca^{2+} (Figure 4). *vma21QQ* yeast cells lacking Voa1p (*voa1::Hyg*^{r} *vma21QQ*) exhibit a severe Ca^{2+} growth defect and fail to acidify their vacuoles, comparable with cells completely lacking V-ATPase. This is consistent with an absence of functional V-ATPase on the vacuole membrane. V_0 domain assembly was severely compromised in *voa1::Hyg*^{r} *vma21QQ* cells, as evidenced by the decreased cellular levels of the V_0 subunit Vph1p and the ER localization of the remaining Vph1p, due to its inability to

assemble into a complete V_0 domain and exit the ER. In addition, ER localization of Voa1p was found to be critical for its function in V_0 domain assembly, because a retrieval-deficient form of Voa1p (Voa1pQQ) could not support V_0 assembly in *voa1::Hyg*^{r} *vma21QQ* cells. The strong enhancement of the Ca^{2+}-sensitive phenotype in *vma21QQ* cells by deletion of Voa1p supports the model that Voa1p functions together with Vma21p in V_0 assembly in the ER.

Characterization of the association of Voa1p with the V_0–Vma21p complex revealed that Voa1p is associated with the partially assembled V_0–Vma21p complex but did not associate significantly with the fully assembled V_0–Vma21p complex found in wild-type cells. Voa1p did not appreciably associate with Vma21p in the absence of the c or c′ components of the core proteolipid ring (composed of subunits c, c′, and c″; Wang *et al*., 2007). This suggests that partial formation of this V_0 core is the minimum requirement for Voa1p association with the Vma21p complex, although the presence of all three components of the proteolipid ring led to the highest level of association. This is corroborated by finding Voa1p most strongly associated with the assembling V_0–Vma21p complex in cells lacking subunit a (*vph1*Δ), subunit d (*vma6*Δ), or subunit e (*vma9*Δ), wherein the full proteolipid ring is associated with Vma21p. Together, these results indicate that Voa1p associates early with the assembling V_0–Vma21p complex in the ER, that it dissociates from the fully assembled V_0-Vma21p complex, and that it does not exit the ER in close association with the V_0–Vma21p complex. In support of these results, a recent proteomics publication reported proximity between Voa1p (YGR106C) and several V-ATPase subunits by using a split DHFR reporter system (Tarassov *et al*., 2008).

V_0 Sector Assembly Pathway

With the identification of Voa1p, the assembly of the V_0 domain in the ER has been shown to be dependent on at least five proteins: Vma12p, Vma21p, Vma22p, Pkr1p, and now Voa1p. Although a specific role for Pkr1p in V_0 assembly has remained elusive (Davis-Kaplan *et al*., 2006), the model in Figure 10 outlines specific roles for the four other proteins in the V_0 assembly pathway. Vma21p associates with subunits c, c′, and c″ to form the core Vma21p–proteolipid ring complex, and loss of neither Vma12p nor Vma22p interferes with the formation of this complex (Malkus *et al*., 2004). Voa1p associates stably with this core Vma21p–proteolipid complex (Figure 10, complex 1). A complex of Vma12p and Vma22p interacts with newly synthesized subunit a (Vph1p; Graham *et al*., 1998) to form complex 2 in the assembly pathway depicted in Figure 10. The addition of subunits a, d, and e to the core Vma21p–proteolipid complex results in the dissociation of the Vma12–22p complex and Voa1p, and the formation of a stable and fully assembled V_0–Vma21p ER-localized complex (Figure 10, complex 3; Malkus *et al*., 2004; Compton *et al*., 2006; this work). The V_0–Vma21p complex is then loaded onto ER-derived coat protein (COP) II vesicles for transport to the *cis*-Golgi. After dissociation of Vma21p from the V_0 domain in the Golgi compartment, COPI-dependent retrieval of Vma21p to the ER (due to Vma21p's C-terminal dilysine motif) allows this assembly/escort factor to function in multiple rounds of V_0 assembly and ER-to-Golgi transport of this essential portion of the V-ATPase complex (Malkus *et al*., 2004).

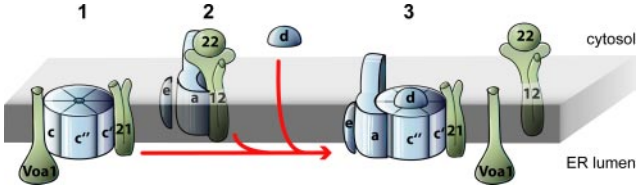

Figure 10. Model of Voa1p function in the assembly of the V-ATPase. Vma21p associates with the V_0 subunits c, c′, and c″ (Vma3p, Vma11p, and Vma16) that assemble to form the proteolipid ring. Voa1p associates with the partially assembled V_0–Vma21p complex in the ER, and this association may be mediated by the proteolipid ring subunits (1). In a parallel assembly pathway, the Vma12p/Vma22p complex interacts with subunit a (Vph1p or Stv1p) (2). The association of Vph1p (subunit a), Vma6p (subunit d), and Vma9p (subunit e) with the proteolipid ring subunits and the dissociation of Voa1p from this complex lead to the formation of the fully assembled V_0–Vma21p complex (3). The fully assembled V_0–Vma21p complex is then competent to exit the ER.

Identifying Additional V-ATPase Assembly/Transport Factors

The intricate pathways, components, and mechanisms of V-ATPase assembly have all been revealed through investigations in the yeast *S. cerevisiae*, and they reflect the ease of forward genetic screens for assembly and regulatory factors that are not stable components of the final V-ATPase complex (Kane, 2006; Forgac, 2007). Interestingly, many of the proteins that regulate V-ATPase assembly and activity have apparent orthologues in higher eukaryotes. Functional orthologues of the yeast V_0 assembly/escort factor Vma21p have been identified recently in plants and animals. *Arabidopsis thaliana* has two apparent Vma21p orthologues (*AtVMA21a* and *AtVMA21b*) with only 25% sequence identity, and they are both capable of functioning in place of the endogenous Vma21p in yeast V-ATPase assembly (Neubert *et al*., 2008). RNA interference knockdown of *Arabidopsis VMA21a* produces phenotypes in plants identical to the elimination of V-ATPase function (Neubert *et al*., 2008). In addition, *Caenorhabditis elegans* has one apparent Vma21p orthologue, and CeVma21p can functionally replace the endogenous Vma21p in yeast V-ATPase assembly (Graham, Black-Maier, and Stevens, unpublished data). Thus, it is highly likely that the V_0 and V_1 domain assembly and V_0–V_1-regulated assembly mechanisms identified in yeast are general for all eukaryotic cells. Proteins similar to Voa1p are present in other fungi (e.g., among the genus of *Kluyveromyces*, *Ashbya*, and *Candida*), and these proteins are predicted to have a similar molecular mass, N-terminal signal sequence and a C-terminal transmembrane sequence. All are uncharacterized ORFs with the exception of *ABG1* from *Candida albicans*. *ABG1* is reported to be an essential gene, and *ABG1* heterozygous and conditional null mutants seem defective in vacuole biogenesis and cytokinesis (Veses *et al*., 2005). Searches of various databases by using the amino acid sequence of Voa1p did not identify any proteins from higher eukaryotes that have significant sequence similarity to Voa1p.

Genetic and genome-wide screens in yeast have identified the numerous proteins that are required for assembly and regulation of the V-ATPase complex (Kane, 2006). The identification of the new V_0 assembly factor Voa1p by proteomic approaches indicates that there may be many additional factors yet to be discovered to fully understand the coordinated assembly of the V_0 domain, the sorting of the V_0–Vma21p complex into COPII vesicles for ER-to-Golgi transport, the selective sorting of the Vph1p-containing and Stv1p-containing V-ATPase complexes, and the regulated dissociation/reassembly of the V_1V_0 complex. *voa1* mutants

would not have been identified in any of the previous V-ATPase/vacuole acidification screens, because its function was only revealed in a compromised genetic background (*vma21QQ*). The identification of proteins such as Voa1p that enhance V_0 assembly (or proteins that have redundant functions) will require enhancer or suppressor screens in sensitized genetic backgrounds (such as *vma21QQ*) to identify mutations that act synthetically with mutations that compromise known factors or to identify proteins that when overexpressed alleviate or exacerbate partial V-ATPase deficiencies. Such approaches will reveal new components of the V-ATPase assembly pathway and help elucidate the detailed mechanism of assembly and regulation of the V-ATPase enzyme complex.

ACKNOWLEDGMENTS

We thank Dave Anderson (University of Oregon) and Phil Gafken and Lisa Nader (Fred Hutchinson Cancer Research Center) for providing mass spectrometry analysis. We also thank members of the Stevens laboratory for helpful comments related to this manuscript. We thank Greg Finnigan for generation of the *vma9*Δ yeast strain and the Vph1p-GFP plasmid used in this work. Additionally we want to thank Mark Compton for time and effort creating the artwork used to generate the final model figure. This work was supported by National Institutes of Health grant GM-38006 (to T.H.S.).

REFERENCES

Ansaldi, M., Lepelletier, M., and MÈjean, V. (1996). Site-specific mutagenesis by using an accurate recombinant polymerase chain reaction method. Anal. Biochem. *234*, 110–111.

Bauerle, C., Ho, M. N., Lindorfer, M. A., and Stevens, T. H. (1993). The *Saccharomyces cerevisiae VMA6* gene encodes the 36-kDa subunit of the vacuolar H^+-ATPase membrane sector. J. Biol. Chem. *268*, 12749–12757.

Bendtsen, J. D., Nielsen, H., von Heijne, G., and Brunak, S. (2004). Improved prediction of signal peptides: SignalP 3.0. J. Mol. Biol. *340*, 783–795.

Beyenbach, K. W., and Wieczorek, H. (2006). The V-type H^+ ATPase: molecular structure and function, physiological roles and regulation. J. Exp. Biol. *209*, 577–589.

Catley, B. J. (1988). Isolation and analysis of cell walls. In: Yeast: A Practical Approach, ed. I. Campell and J. H. Duffus, Oxford, England: IRL Press, 163–183.

Compton, M. A., Graham, L. A., and Stevens, T. H. (2006). Vma9p (subunit e) is an integral membrane V_0 subunit of the yeast V-ATPase. J. Biol. Chem. *281*, 15312–15319.

Conibear, E., and Stevens, T. H. (2002). Studying yeast vacuoles. Methods Enzymol. *351*, 408–432.

Craig, R., and Beavis, R. C. (2004). TANDEM: matching proteins with tandem mass spectra. Bioinformatics *20*, 1466–1467.

Curtis, K. K., and Kane, P. M. (2002). Novel vacuolar H^+-ATPase complexes resulting from overproduction of Vma5p and Vma13p. J. Biol. Chem. *277*, 2716–2724.

Davis-Kaplan, S. R., Compton, M. A., Flannery, A. R., Ward, D. M., Kaplan, J., Stevens, T. H., and Graham, L. A. (2006). PKR1 encodes an assembly factor for the yeast V-type ATPase. J. Biol. Chem. *281*, 32025–32035.

Doherty, R. D., and Kane, P. M. (1993). Partial assembly of the yeast vacuolar H^+-ATPase in mutants lacking one subunit of the enzyme. J. Biol. Chem. *268*, 16845–16851.

Flannery, A. R., Graham, L. A., and Stevens, T. H. (2004). Topological characterization of the c, c′, and c′′ subunits of the vacuolar ATPase from the yeast *Saccharomyces cerevisiae*. J. Biol. Chem. *279*, 39856–39862.

Forgac, M. (2007). Vacuolar ATPases: rotary proton pumps in physiology and pathophysiology. Nat. Rev. Mol. Cell Biol. *8*, 917–929.

Fujiki, Y., Hubbard, A. L., Fowler, S., and Lazarow, P. B. (1982). Isolation of intracellular membranes by means of sodium carbonate treatment: application to endoplasmic reticulum. J. Cell Biol. *93*, 97–102.

Goldstein, A. L., and McCusker, J. H. (1999). Three new dominant drug resistance cassettes for gene disruption in *Saccharomyces cerevisiae*. Yeast *15*, 1541–1553.

Graham, L. A., Flannery, A. R., and Stevens, T. H. (2003). Structure and assembly of the yeast V-ATPase. J. Bioenerg. Biomembr. *35*, 301–312.

Graham, L. A., Hill, K. J., and Stevens, T. H. (1998). Assembly of the yeast vacuolar H^+-ATPase occurs in the endoplasmic reticulum and requires a Vma12p/Vma22p assembly complex. J. Cell Biol. *142*, 39–49.

Hill, K. J., and Stevens, T. H. (1994). Vma21p is a yeast membrane protein retained in the endoplasmic reticulum by a di-lysine motif and is required for the assembly of the vacuolar H^+-ATPase complex. Mol. Biol. Cell *5*, 1039–1050.

Hill, K. J., and Stevens, T. H. (1995). Vma22p is a novel endoplasmic reticulum associated protein required for assembly of the yeast vacuolar H^+-ATPase complex. J. Biol. Chem. *270*, 22329–22336.

Hirata, R., Umemoto, N., Ho, M. N., Ohya, Y., Stevens, T. H., and Anraku, Y. (1993). VMA12 is essential for assembly of the vacuolar H^+-ATPase subunits onto the vacuolar membrane in *Saccharomyces cerevisiae*. J. Biol. Chem. *268*, 961–967.

Hirata, T., Iwamoto-Kihara, A., Sun-Wada, G. H., Okajima, T., Wada, Y., and Futai, M. (2003). Subunit rotation of vacuolar-type proton pumping ATPase: relative rotation of the G as to c subunit. J. Biol. Chem. *278*, 23714–23719.

Hirokawa, T., Boon-Chieng, S., and Mitaku, S. (1998). SOSUI: classification and secondary structure prediction system for membrane proteins. Bioinformatics *14*, 378–379.

Imamura, H., Nakano, M., Noji, H., Muneyuki, E., Ohkuma, S., Yoshida, M., and Yokoyama, K. (2003). Evidence for rotation of V_1-ATPase. Proc. Natl. Acad. Sci. USA *100*, 2312–2315.

Jackson, D. D., and Stevens, T. H. (1997). VMA12 encodes a yeast endoplasmic reticulum protein required for vacuolar H^+-ATPase assembly. J. Biol. Chem. *272*, 25928–25934.

Kaiser, C. A., Chen, E. J., and Losko, S. (2002). Subcellular fractionation of secretory organelles. Methods Enzymol. *351*, 325–338.

Kane, P. M. (2006). The where, when, and how of organelle acidification by the yeast vacuolar H^+-ATPase. Microbiol. Mol. Biol. Rev. *70*, 177–191.

Kane, P. M., Tarsio, M., and Liu, J. (1999). Early steps in assembly of the yeast vacuolar H^+-ATPase. J. Biol. Chem. *274*, 17275–17283.

Kawasaki-Nishi, S., Bowers, K., Nishi, T., Forgac, M., and Stevens, T. H. (2001). The amino-terminal domain of the vacuolar proton-translocating ATPase a subunit controls targeting and in vivo dissociation, and the carboxyl-terminal domain affects coupling of proton transport and ATP hydrolysis. J. Biol. Chem. *276*, 47411–47420.

Keller, A., Nesvizhskii, A. I., Kolker, E., and Aebersold, R. (2002). Empirical statistical model to estimate the accuracy of peptide identifications made by MS/MS and database search. Anal. Chem. *74*, 5383–5392.

Kitagawa, N., Mazon, H., Heck, A. J., and Wilkens, S. (2008). Stoichiometry of the peripheral stalk subunits E and G of yeast V_1-ATPase determined by mass spectrometry. J. Biol. Chem. *283*, 3329–3337.

Liu, J. Z., and Kane, P. M. (1996). Mutational analysis of the catalytic subunit of the yeast vacuolar proton-translocating ATPase. Biochemistry *35*, 10938–10948.

Liu, Q., Kane, P. M., Newman, P. R., and Forgac, M. (1996). Site-directed mutagenesis of the yeast V-ATPase B subunit (Vma2p). J. Biol. Chem. *271*, 2018–2022.

MacLean, B., Eng, J. K., Beavis, R. C., and McIntosh, M. (2006). General framework for developing and evaluating database scoring algorithms using the TANDEM search engine. Bioinformatics *22*, 2830–2832.

Malkus, P., Graham, L. A., Stevens, T. H., and Schekman, R. (2004). Role of Vma21p in assembly and transport of the yeast vacuolar ATPase. Mol. Biol. Cell *15*, 5075–5091.

Manolson, M. F., Proteau, D., Preston, R. A., Stenbit, A., Roberts, B. T., Hoyt, M. A., Preuss, D., Mulholland, J., Botstein, D., and Jones, E. W. (1992). The *VPH1* gene encodes a 95-kDa integral membrane polypeptide required for *in vivo* assembly and activity of the yeast vacuolar H^+-ATPase. J. Biol. Chem. *267*, 14294–14303.

Manolson, M. F., Wu, B., Proteau, D., Taillon, B. E., Roberts, B. T., Hoyt, M. A., and Jones, E. W. (1994). STV1 gene encodes functional homologue of the 95-kDa yeast vacuolar H^+-ATPase subunit Vph1p. J. Biol. Chem. *269*, 14064–14074.

Neubert, C., Graham, L. A., Black-Maier, E. W., Coonrod, E. M., Liu, T. Y., Stierhof, Y. D., Seidel, T., Stevens, T. H., and Schumacher, K. (2008). *Arabidopsis* has two functional orthologs of the yeast V-ATPase assembly factor Vma21p. Traffic *9*, 1618–1628.

Ohira, M., Smardon, A. M., Charsky, C. M., Liu, J., Tarsio, M., and Kane, P. M. (2006). The E and G subunits of the yeast V-ATPase interact tightly and are both present at more than one copy per V_1 complex. J. Biol. Chem. *281*, 22752–22760.

Powell, B., Graham, L. A., and Stevens, T. H. (2000). Molecular characterization of the yeast vacuolar H^+-ATPase proton pore. J. Biol. Chem. *275*, 23654–23660.

Rauch, A. *et al*. (2006). Computational Proteomics Analysis System (CPAS): an extensible, open-source analytic system for evaluating and publishing proteomic data and high throughput biological experiments. J. Proteome Res. *5*, 112–121.

Rothman, J. H., and Stevens, T. H. (1986). Protein sorting in yeast: mutants defective in vacuole biogenesis mislocalize vacuolar proteins into the late secretory pathway. Cell *47*, 1041–1051.

Sambrook, J., and Russel, D. W. (2001). Molecular Cloning: A Laboratory Manual, 3rd ed., Cold Spring Harbor, NY: Cold Spring Harbor Laboratory Press.

Seol, J. H., Shevchenko, A., Shevchenko, A., and Deshaies, R. J. (2001). Skp1 forms multiple protein complexes, including RAVE, a regulator of V-ATPase assembly. Nat. Cell Biol. *3*, 384–391.

Shevchenko, A., Wilm, M., Vorm, O., and Mann, M. (1996). Mass spectrometric sequencing of proteins silver-stained polyacrylamide gels. Anal. Chem. *68*, 850–858.

Sikorski, R. S., and Hieter, P. (1989). A system of shuttle vectors and yeast host strains designed for efficient manipulation of DNA in *Saccharomyces cerevisiae*. Genetics *122*, 19–27.

Smardon, A. M., and Kane, P. M. (2007). RAVE is essential for the efficient assembly of the C subunit with the vacuolar H^+-ATPase. J. Biol. Chem. *282*, 26185–26194.

Smardon, A. M., Tarsio, M., and Kane, P. M. (2002). The RAVE complex is essential for stable assembly of the yeast V-ATPase. J. Biol. Chem. *277*, 13831–13839.

Tarassov, K., Messier, V., Landry, C. R., Radinovic, S., Molina, M. M., Shames, I., Malitskaya, Y., Vogel, J., Bussey, H., and Michnick, S. W. (2008). An in vivo map of the yeast protein interactome. Science *320*, 1465–1470.

Uchida, E., Ohsumi, Y., and Anraku, Y. (1985). Purification and properties of H^+-translocating, Mg^{+2}-adenosine triphosphatase from vacuolar membranes of *Saccharomyces cerevisiae*. J. Biol. Chem. *260*, 1090–1095.

Veses, V., Casanova, M., Murgui, A., Dominguez, A., Gow, N. A., and Martinez, J. P. (2005). ABG1, a novel and essential *Candida albicans* gene encoding a vacuolar protein involved in cytokinesis and hyphal branching. Eukaryot. Cell *4*, 1088–1101.

Wang, Y., Cipriano, D. J., and Forgac, M. (2007). Arrangement of subunits in the proteolipid ring of the V-ATPase. J. Biol. Chem. *282*, 34058–34065.

Weisman, L. S., Bacallao, R., and Wickner, W. (1987). Multiple methods of visualizing the yeast vacuole permit evaluation of its morphology and inheritance during the cell cycle. J. Cell Biol. *105*, 1539–1547.

Yi, E. C., Lee, H., Aebersold, R., and Goodlett, D. R. (2003). A microcapillary trap cartridge-microcapillary high-performance liquid chromatography electrospray ionization emitter device capable of peptide tandem mass spectrometry at the attomole level on an ion trap mass spectrometer with automated routine operation. Rapid Commun. Mass Spectrom. *17*, 2093–2098.

Yokoyama, K., Nakano, M., Imamura, H., Yoshida, M., and Tamakoshi, M. (2003). Rotation of the proteolipid ring in the V-ATPase. J. Biol. Chem. *278*, 24255–24258.

Zheng, L., Baumann, U., and Reymond, J. L. (2004). An efficient one-step site-directed and site-saturation mutagenesis protocol. Nucleic Acids Res. *32*, e115